

# Determination of Electric and Magnetic Field Calculation Uncertainty in the Vicinity of Overhead Transmission Lines

Ajdin Alihodzic , Adnan Mujezinovic , Emir Turajlic , Maja Muftic Dedovic   
Faculty of Electrical Engineering, University of Sarajevo, Sarajevo, Bosnia and Herzegovina  
[ajdin.alihodzic@etf.unsa.ba](mailto:ajdin.alihodzic@etf.unsa.ba), [adnan.mujezinovic@etf.unsa.ba](mailto:adnan.mujezinovic@etf.unsa.ba), [eturajlic@etf.unsa.ba](mailto:eturajlic@etf.unsa.ba),  
[maja.muftic-dedovic@etf.unsa.ba](mailto:maja.muftic-dedovic@etf.unsa.ba)

**Abstract**— This paper presents a new approach for uncertainty determination of the electric field intensity and magnetic flux density calculation in the vicinity of overhead transmission lines. The proposed method is based on the law of propagation of uncertainty as defined in the Guide to the expression of Uncertainty in Measurement. A mathematical model is developed for determining the electric field intensity and magnetic flux density calculation uncertainty based on the Charge simulation method and method based on Biot – Savart law, respectively. The verification of the proposed method was performed by estimating the uncertainty of the electric field and magnetic flux density calculations for four single circuit and two double circuit high-voltage overhead transmission lines. The analysis of the obtained results demonstrates that the proposed method can be successfully used to determine the uncertainty of electric field intensity and magnetic flux density calculations in the vicinity of overhead transmission lines.

**Index Terms**— Biot-Savart (BS) law based method, Charge simulation method (CSM), Electric field intensity, Law of propagation of uncertainty, Magnetic flux density.

## I. INTRODUCTION

With the development of industry and rising living standards, the demands for electricity have increased, which requires the development of electric power systems to meet all the requirements. The electricity demands cannot be met without the penetration of electric powers system infrastructure deep into urban areas, leading to direct exposure of the population to their impacts. When designing new transmission lines, it is necessary to take into account numerous constraints, such as capacity limits, safety distances, maximum allowable electric and magnetic fields, noise levels, etc. [1]–[4]. Furthermore, it is important to verify that these aforementioned constraints are also satisfied by the overhead transmission lines that are already in operation.

In recent decades, a significant research effort is made to better understand the possible effects of electric and magnetic fields on people living in the vicinity of overhead transmission lines. Since various epidemiological studies have established a statistical association between the exposure to the electric and magnetic fields and the incidences of severe diseases, the primary goal of these limit values is to prevent the occurrence of induced currents in the human body that are higher than currents in the nervous system and heart [5]–[7]. In 2010, The International Commission on Non-Ionizing Radiation Protection (ICNIRP) has published guidelines for limiting exposure to time-varying electric and magnetic fields

in the frequency range from 1 Hz to 100 kHz. According to these guidelines, the reference levels are 10 kV/m and 1 mT for occupational exposure to 50 Hz electric and magnetic fields and 5 kV/m and 0.2 mT for general public exposure [8].

Although the guidelines and regulations provide recommendations on acceptable values of electric and magnetic fields, they do not provide instructions on how to verify compliance with the prescribed limits. In case of power facilities that are already in operation, the compliance with the prescribed limits can be verified by the field calculation or measurement results [9]. On the other hand, when it comes to power facilities that have not yet been build, during the design phase, the electric field intensity and magnetic flux density calculation results are used to ensure that the power facilities comply with the prescribed values.

Numerous analytical and numerical methods have been developed to calculate electric field intensity and magnetic flux density in the vicinity of power system infrastructure (such as overhead transmission lines and substations). Popular methods for analytical calculation of electric field intensity and magnetic flux density are based on multi pole expansion [10] and Biot-Savart (BS) law [11], respectively. The most commonly used numerical calculation methods are charge simulation method (CSM), finite element method (FEM), boundary element method (BEM) and surface charge simulation method (SCSM) [12].

Due to the ease of understanding and programming, the most commonly used method for calculating overhead transmission line electric field intensity is CSM [13]. In an effort to improve its performance, over the years various variants of CSM have been proposed. On the other hand, the calculation of the magnetic flux density in the proximity of overhead transmission lines is most commonly based on the Biot-Savart law [14].

Regardless of how the electric field intensity and magnetic flux density values are obtained, by measurements or calculations, the analysis of these results and any conclusions that are based on these results should take into account the measurement and calculation uncertainties.

In general, the observed discrepancies between the measurement and calculation results are associated with the measurement and calculation uncertainties [15]. Uncertainty is defined as a quantitative measure of measurement or calculation quality. As such, it is necessary to evaluate uncertainty in a consistent and a generally accepted manner. These requirements associated with the uncertainty evaluation are discussed in the Guide on the Expression of Uncertainty in Measurement (GUM) [16]. Uncertainty evaluation is based on incomplete knowledge of the measurements and calculations used, as well as the values of the input parameters that affect the output quantity. The calculations can be regarded as virtual experiments and it is necessary to express the uncertainty associated with the obtained results [17].

The quantification of uncertainty results from the fact that the results of measurements, calculations and experiments are taken with a certain doubt in their accuracy. Some of the scenarios in which uncertainty is expressed are: comparison of measured data and results of numerical simulations, comparison of calculation or measurement results with limits and tolerances defined by standards, or with theoretical considerations and analytical results, interlaboratory comparisons [18], [19]. In GUM, measurement uncertainty is defined as a parameter associated with the measurement results, which characterizes the scatter of values that may be associated with the measured quantity [16].

In particular, the evaluation of uncertainty becomes significant when examining compliance with the guidelines and limits for limiting human exposure to electric and magnetic fields. When determining

measurement uncertainty, several problems are encountered, and the most important are the identification and quantification of all uncertainty components [20], [21].

When it comes to calculations of electric field intensity and magnetic flux density near overhead transmission lines, the choice of calculation method and the input data uncertainty affects the overall results uncertainty. The input data constitute overhead transmission line geometry and applied voltage and current intensity values. When calculations of electric field intensity and magnetic flux density of overhead transmission lines in operation are performed, for some precisely determined conditions, the applied voltage and current values are obtained using voltage and current measuring transformers. Thus, these values are accompanied by measurement uncertainty that depends on the accuracy class of the instruments [15], [22]. The geometry of the overhead transmission line, and specifically the conductor heights are obtained by measurement. These measurements should be performed at minimum conductor height, where highest field values are expected [23]. The accuracy of these measurements depends on the declared accuracy of the used instrument and the way in which the operator performs the measurement procedure.

In this paper, a method for determination of the electric field intensity and magnetic flux density calculation uncertainty in the vicinity of overhead transmission lines is proposed. The proposed method is based on the law of propagation of uncertainty, defined in GUM. Since the CSM and BS law based methods are the most commonly used for the electric field intensity and magnetic flux density calculations, respectively, a mathematical model is developed to determine their corresponding calculation uncertainties.

The rest of the paper is organized as follows. Section II gives a detailed description of the proposed method. In this section, a mathematical model for electric field intensity and magnetic flux density calculation uncertainty is developed. In Section III, the proposed method is applied on four single circuit and two double circuit overhead transmission lines. Obtained results, together with the corresponding discussion are presented within this section. Section IV concludes the paper.

## II. MATHEMATICAL MODEL

The problem of quantifying uncertainty of field measurements is treated in GUM, scientific and professional literature, but this is not the case with the uncertainty of calculation procedures [16]. In this paper, starting from the law of propagation of uncertainty, given in GUM, a mathematical model is developed for determining the uncertainty of the calculation of electric field intensity and magnetic flux density in the vicinity of overhead transmission lines based on the CSM method and BS law-based method, respectively. The proposed model considers the uncertainties associated with the following input data: applied voltage, current intensity, and conductor heights. In this paper, it is assumed that voltage and current intensity measurement uncertainties correspond to ratio errors of voltage and current measuring transformers, while the uncertainty of height measurement is obtained from the manufacturer instrument specification. The horizontal coordinates of conductors are taken from technical documentation without expressing their uncertainties.

The starting position for any uncertainty analysis is a mathematical model of calculation or measurement method. Most often, the quantity of interest cannot be determined directly, but as a function of  $n$  other quantities  $X_1, \dots, X_n$ :

$$y = f(X_1, \dots, X_n) \quad (1)$$

If the input quantities can be represented as independent random variables, then the combined standard uncertainty is defined as:

$$u_y = \sqrt{\sum_{i=1}^n \left(\frac{\partial f}{\partial x_i}\right)^2 \cdot (u_{x_i})^2} \quad (2)$$

where  $f$  is a function defined by equation (1),  $\partial$  is derivative operator,  $u_{x_i}$  is standard uncertainty of a  $i$ -th input quantity, and  $\frac{\partial f}{\partial x_i}$  denotes sensitivity coefficients which are defined as partial derivative of function  $f$  with respect to  $i$ -th quantity.

Combined standard uncertainty, denoted by  $u_y$ , is the estimated standard deviation and characterizes the dispersion of values that can be reasonably associated with the magnitude of interest [16], [18].

#### A. Electric field intensity uncertainty calculation

In this paper, 2D algorithm of the CSM method is used for the calculation of the electric field intensity, since it is most commonly used for electric field intensity calculations. The electric field intensity vector at an arbitrary point  $P(y, z)$ , in the vicinity of an overhead transmission line, can be decomposed into independent spatial phasor components:

$$\vec{E} = \{E_y, E_z\} \quad (3)$$

With respect to CSM method, the overhead transmission lines are considered as an appropriate number of fictitious point charge sources positioned in an infinite air half-space. In this paper, each phase conductor and shielding wire is represented by one fictitious point charge. Unknown fictitious point charges can be calculated by (4) [24].

$$\{q\} = [P]^{-1} \cdot \{U\} \quad (4)$$

where  $\{U\}$  is line-to-ground voltage phasors matrix,  $\{q\}$  is matrix of the unknown fictitious point charge phasors and  $[P]$  represents matrix of potential coefficients.

Since each conductor is represented by one fictitious point charge, different equations are used to calculate the self and mutual coefficients of the matrix of potential coefficients. For overhead transmission lines, which consist of  $n$  parallel conductors, the self and mutual elements of the potential coefficients matrix are given by (5) and (6).

$$P_{ii} = \frac{1}{2\pi \cdot \varepsilon_0} \cdot \ln \frac{2 \cdot z_i}{R_i} \quad (5)$$

$$P_{ij} = \frac{1}{2\pi \cdot \varepsilon_0} \cdot \ln \frac{D_{ij}}{d_{ij}} \quad (6)$$

where  $\varepsilon_0$  denotes the dielectric constant of air,  $z_i$  is vertical coordinate of the  $i$ -th conductor,  $R_i$  is the radius of the  $i$ -th conductor,  $d_{ij}$  is the shortest distance between  $i$ -th and  $j$ -th conductor and  $D_{ij}$  is the shortest distance between  $i$ -th conductor and the image of  $j$ -th conductor, as shown in Fig. 1.

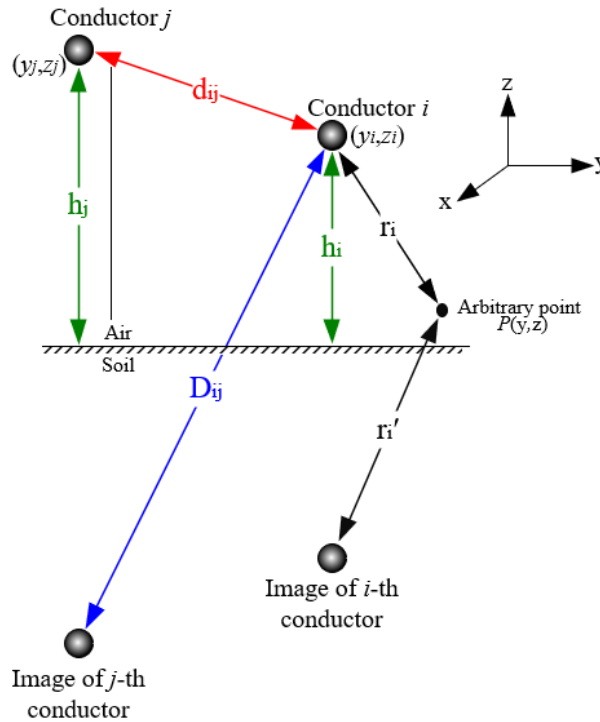


Fig. 1. The distances between the point charges, the image of point charges and an arbitrary point [24]

It can be noted that the phasors of the fictitious point charges, as defined by (4), are functions of the applied line-to-ground voltage phasors and conductor heights. Therefore, following equation can be written:

$$q_i = f(\underline{U}_1, \dots, \underline{U}_n, z_1, \dots, z_n) \quad (7)$$

By applying the law of propagation of uncertainty, i.e. (2), to the calculation of fictitious point charges, as indirectly determined quantities, dependent on the voltage and height of each individual conductor, the uncertainties of the calculation of individual point charges are determined as follows:

$$u_{q_i} = \sqrt{\sum_{i=1}^n \left( \frac{\partial q_i}{\partial \underline{U}_i} \right)^2 \cdot (u_{U_i})^2 + \sum_{i=1}^n \left( \frac{\partial q_i}{\partial z_i} \right)^2 \cdot (u_{z_i})^2} \quad (8)$$

where  $u_{q_i}$  represents uncertainty of  $i$ -th fictitious charge calculation,  $u_{U_i}$  denotes uncertainty of voltage measurement for  $i$ -th conductor, and  $u_{z_i}$  is uncertainty of height measurement of  $i$ -th conductor.

Voltage and height measurement uncertainties are defined as measurement uncertainty of type B. This type of uncertainty of described in detail in GUM [16].

Sensitivity coefficients for determining the uncertainty of the calculation of fictitious point charges are defined as partial derivatives of fictitious point charges with respect to the voltages and the heights of individual conductors, as follows:

$$\left\{ \frac{\partial q}{\partial \underline{U}_i} \right\} = [P]^{-1} \cdot \left\{ \frac{\partial U}{\partial \underline{U}_i} \right\} \quad (9)$$

$$\left\{ \frac{\partial q}{\partial z_i} \right\} = \left[ \frac{\partial P}{\partial z_i} \right]^{-1} \cdot \{U\} \quad (10)$$

In order to simplify (9) and (10), it is convenient to use the following rule [25]:

$$\left[ \frac{\partial P}{\partial z_i} \right]^{-1} = -[P]^{-1} \cdot \left[ \frac{\partial P}{\partial z_i} \right] \cdot [P]^{-1} \quad (11)$$

Thus, when the rule defined in (11) is applied to (10), the following expression for sensitivity coefficients is obtained:

$$\left\{ \frac{\partial \underline{q}}{\partial z_i} \right\} = -[P]^{-1} \cdot \left[ \frac{\partial P}{\partial z_i} \right] \cdot [P]^{-1} \cdot \{ \underline{U} \} \quad (12)$$

Since the matrix of potential coefficients is defined by (5) and (6), potential coefficient derivatives matrix is also defined by two equations. The self and mutual elements (main diagonal and off-diagonal elements) of potential coefficient derivatives matrix are defined as:

$$\frac{\partial P_{ii}}{\partial z_i} = \frac{1}{2\pi \cdot \epsilon_0} \cdot \frac{1}{z_i} \quad (13)$$

$$\frac{\partial P_{ij}}{\partial z_i} = \frac{1}{2\pi \cdot \epsilon_0} \cdot \frac{2 \cdot z_j \cdot [(y_i - y_j)^2 - z_i^2 + z_j^2]}{[(y_i - y_j)^2 + (z_i - z_j)^2] \cdot [(y_i - y_j)^2 + (z_i + z_j)^2]} \quad (14)$$

The electric field intensity components at an arbitrary point produced by  $n$  fictitious point charges is calculated using the following equations [26]:

$$\underline{E}_y(y, z) = \sum_{i=1}^n \frac{q_i}{2\pi \cdot \epsilon_0} \cdot \left( \frac{y - y_i}{r_i^2} + \underline{\Gamma} \frac{y - y_i}{r_i'^2} \right) \quad (15)$$

$$\underline{E}_z(y, z) = \sum_{i=1}^n \frac{q_i}{2\pi \cdot \epsilon_0} \cdot \left( \frac{z - z_i}{r_i^2} + \underline{\Gamma} \frac{z + z_i}{r_i'^2} \right) \quad (16)$$

where  $(y, z)$  are coordinates of an arbitrary point,  $(y_i, z_i)$  are coordinates of the  $i$ -th fictitious point charge,  $r_i$  is the shortest distance between the  $i$ -th fictitious point charge and the arbitrary point,  $r_i'$  is the shortest distance between complex image of the  $i$ -th fictitious point charge and the arbitrary point, as shown in Fig. 1. The parameter  $\underline{\Gamma}$  represents the reflection coefficient which takes into account the influence of the soil surface on the calculation of the electric field intensity components at an arbitrary point. Often, the reflection coefficient value  $\underline{\Gamma} \approx -1$  is used [24].

From the previous analysis, it is clear that the horizontal and vertical components of the electric field intensity are functions of fictitious point charges and the heights at which individual conductors are located. Therefore, following can be written:

$$\underline{E}_y(y, z) = f(\underline{q}_1, \dots, \underline{q}_n, z_1, \dots, z_n) \quad (17)$$

$$\underline{E}_z(y, z) = f(\underline{q}_1, \dots, \underline{q}_n, z_1, \dots, z_n) \quad (18)$$

Following the previously introduced principle, the uncertainties of calculation of the horizontal and vertical electric field intensity components are determined as follows:

$$\underline{u}_{E_y}(y, z) = \sqrt{\sum_{i=1}^n \left( \frac{\partial \underline{E}_y(y, z)}{\partial q_i} \right)^2 \cdot (u_{q_i})^2 + \sum_{i=1}^n \left( \frac{\partial \underline{E}_y(y, z)}{\partial z_i} \right)^2 \cdot (u_{z_i})^2} \quad (19)$$

$$\underline{u}_{E_z}(y, z) = \sqrt{\sum_{i=1}^n \left( \frac{\partial \underline{E}_z(y, z)}{\partial q_i} \right)^2 \cdot (u_{q_i})^2 + \sum_{i=1}^n \left( \frac{\partial \underline{E}_z(y, z)}{\partial z_i} \right)^2 \cdot (u_{z_i})^2} \quad (20)$$

where  $\underline{u}_{E_y}(y, z)$  and  $\underline{u}_{E_z}(y, z)$  are uncertainties of calculation of horizontal and vertical components of the electric field intensity at an arbitrary point with the coordinates  $P(y, z)$ , respectively.

In order to calculate the uncertainties associated with horizontal and vertical components of the electric field intensity, as defined in (19) and (20), it is necessary to determine the sensitivity coefficients. Sensitivity coefficients represent the partial derivatives of the electric field intensity function at an arbitrary point with respect to fictitious point charge phasors and partial derivatives of electric field intensity function with respect to conductor heights. The sensitivity coefficients are defined by:

$$\frac{\partial \underline{E}_y(y, z)}{\partial q_i} = \frac{1}{2\pi \cdot \epsilon_0} \cdot \left( \frac{y - y_i}{r_i^2} + \Gamma \frac{y - y_i}{r_i'^2} \right) \quad (21)$$

$$\frac{\partial \underline{E}_z(y, z)}{\partial q_i} = \frac{1}{2\pi \cdot \epsilon_0} \cdot \left( \frac{z - z_i}{r_i^2} + \Gamma \frac{z + z_i}{r_i'^2} \right) \quad (22)$$

$$\frac{\partial \underline{E}_y(y, z)}{\partial z_i} = \frac{q_i}{2\pi \cdot \epsilon_0} \cdot \left( \frac{2(y - y_i)(z - z_i)}{[(y - y_i)^2 + (z - z_i)^2]^2} - \Gamma \frac{2(y - y_i)(z + z_i)}{[(y - y_i)^2 + (z + z_i)^2]^2} \right) \quad (23)$$

$$\frac{\partial \underline{E}_z(y, z)}{\partial z_i} = \frac{q_i}{2\pi \cdot \epsilon_0} \cdot \left( \frac{\Gamma}{[(z + z_i)^2 + (y - y_i)^2]} - \frac{2\Gamma(z + z_i)^2}{[(z + z_i)^2 + (y - y_i)^2]^2} + \frac{2(z - z_i)^2}{[(z - z_i)^2 + (y - y_i)^2]^2} - \frac{1}{[(z - z_i)^2 + (y - y_i)^2]} \right) \quad (24)$$

Partial derivatives with respect to conductor heights are derived under assumption that vertical coordinate of  $i$ -th conductor image is equal in value but with opposite sign in regards to  $i$ -th conductor vertical coordinate, which results from the application of the image theory.

The resultant value of electric field intensity at an arbitrary point  $P(y, z)$  is determined using (25).

$$E(y, z) = \sqrt{\left| \underline{E}_y(y, z) \right|^2 + \left| \underline{E}_z(y, z) \right|^2} \quad (25)$$

According to the law of propagation of uncertainty, the magnitude of electric field intensity uncertainty vector at an arbitrary point  $P(y, z)$  can be calculated using (26)

$$u_E(y, z) = \sqrt{\left| \underline{u}_{E_y}(y, z) \right|^2 + \left| \underline{u}_{E_z}(y, z) \right|^2} \quad (26)$$

Finally, the electric field intensity expanded uncertainty band at an arbitrary point  $P(x, y)$  can be calculated using (27).

$$E_{band}(y, z) = E(y, z) \pm k \cdot u_E(y, z) = E(y, z) \pm U_E(y, z) \quad (27)$$

where  $k = \sqrt{3}$  denotes the coverage factor,  $U_E(y, z)$  represents the expanded uncertainty of electric field intensity at an arbitrary point.

### B. Magnetic flux density uncertainty calculation

For the calculation of the magnetic flux density in the proximity of overhead transmission line 2D algorithm based on Biot-Savart law is used. Thus, at an arbitrary point  $P(y, z)$ , the magnetic flux density spatial phasor components are defined as [14]:

$$\underline{B}_y(y, z) = \sum_{i=1}^n \frac{\mu_0 \cdot \underline{I}_i}{2\pi} \cdot \left( -\frac{z - z_i}{r_i^2} + \frac{z + z_i + \underline{\alpha}}{r_i'^2} \right) \quad (28)$$

$$\underline{B}_z(y, z) = \sum_{i=1}^n \frac{\mu_0 \cdot \underline{I}_i}{2\pi} \cdot \left( \frac{y - y_i}{r_i^2} - \frac{y - y_i}{r_i'^2} \right) \quad (29)$$

where  $\mu_0$  denotes magnetic permeability of air,  $n$  is total number of the current point sources,  $\underline{I}_i$  is phasor of current intensity of  $i$ -th current source. The coefficient  $\underline{\alpha}$  takes into account the presence of ground surface according to the complex image theory and can be calculated by the following equation [27]:

$$\underline{\alpha} = \frac{2}{\sqrt{-j \cdot \omega \cdot \mu_0 \cdot (\sigma_{soil} - j \cdot \omega \cdot \varepsilon_{soil})}} \quad (30)$$

where  $j$  represents imaginary unit,  $\omega$  is power system angular frequency,  $\sigma_{soil}$  is soil conductivity and  $\varepsilon_{soil}$  is dielectric constant of the soil.

The spatial components of the magnetic flux density are functions of the conductor current intensities and the conductor heights. Therefore, the magnetic flux density components at arbitrary point  $P(y, z)$  can be represented by the following functions:

$$\underline{B}_y(y, z) = f(\underline{I}_1, \dots, \underline{I}_n, z_1, \dots, z_n) \quad (31)$$

$$\underline{B}_z(y, z) = f(\underline{I}_1, \dots, \underline{I}_n, z_1, \dots, z_n) \quad (32)$$

According to (2), the uncertainties of the horizontal and vertical components of the magnetic flux density are functions of the input parameters uncertainties. Therefore, the uncertainties of magnetic flux density components are calculated using (33) and (34).

$$\underline{u}_{B_y}(y, z) = \sqrt{\sum_{i=1}^n \left( \frac{\partial \underline{B}_y(y, z)}{\partial \underline{I}_i} \right)^2 \cdot (\underline{u}_{I_i})^2 + \sum_{i=1}^n \left( \frac{\partial \underline{B}_y(y, z)}{\partial z_i} \right)^2 \cdot (u_{z_i})^2} \quad (33)$$

$$\underline{u}_{B_z}(y, z) = \sqrt{\sum_{i=1}^n \left( \frac{\partial \underline{B}_z(y, z)}{\partial \underline{I}_i} \right)^2 \cdot (\underline{u}_{I_i})^2 + \sum_{i=1}^n \left( \frac{\partial \underline{B}_z(y, z)}{\partial z_i} \right)^2 \cdot (u_{z_i})^2} \quad (34)$$

where  $\underline{u}_{B_y}(y, z)$  and  $\underline{u}_{B_z}(y, z)$  are uncertainties of individual spatial magnetic flux density components at an arbitrary point  $P(y, z)$ , and  $\underline{u}_{I_i}$  denotes the  $i$ -th conductor current intensity measurement uncertainty.

In order to calculate the uncertainties of magnetic flux density components it is necessary to determine the sensitivity coefficients that appear in (33) and (34). These sensitivity coefficients at an arbitrary point represent the partial derivatives of magnetic flux density function with respect to current intensity phasors and partial derivatives of magnetic flux density function with respect to conductor heights. The sensitivity coefficients are defined by (35)-(38).

$$\frac{\partial \underline{B}_y(y, z)}{\partial \underline{I}_i} = \frac{\mu_0}{2\pi} \cdot \left( -\frac{z - z_i}{r_i^2} + \frac{z + z_i + \alpha}{r_i'^2} \right) \quad (35)$$

$$\frac{\partial \underline{B}_z(y, z)}{\partial \underline{I}_i} = \frac{\mu_0}{2\pi} \cdot \left( \frac{y - y_i}{r_i^2} - \frac{y - y_i}{r_i'^2} \right) \quad (36)$$

$$\frac{\partial \underline{B}_y(y, z)}{\partial z_i} = \frac{\mu_0 \cdot \underline{I}_i}{2\pi} \cdot \left( \frac{1}{[(z + z_i)^2 + (y - y_i)^2]} - \frac{2 \cdot (z + z_i) \cdot (z + z_i + \alpha)}{[(z + z_i)^2 + (y - y_i)^2]^2} + \frac{2 \cdot (z - z_i) \cdot (z_i - z)}{[(z - z_i)^2 + (y - y_i)^2]^2} + \frac{1}{[(z - z_i)^2 + (y - y_i)^2]} \right) \quad (37)$$

$$\frac{\partial \underline{B}_z(y, z)}{\partial z_i} = \frac{\mu_0 \cdot \underline{I}_i}{2\pi} \cdot \left( \frac{2 \cdot (y - y_i) \cdot (z + z_i)}{[(y - y_i)^2 + (z + z_i)^2]^2} + \frac{2 \cdot (y - y_i) \cdot (z - z_i)}{[(y - y_i)^2 + (z - z_i)^2]^2} \right) \quad (38)$$

The resultant magnetic flux density value at an arbitrary point  $P(y, z)$  is determined from the magnetic flux density components by (39).

$$B(y, z) = \sqrt{\left| \underline{B}_y(y, z) \right|^2 + \left| \underline{B}_z(y, z) \right|^2} \quad (39)$$

According to the law of propagation of uncertainty, the magnitude of magnetic flux density uncertainty vector at an arbitrary point  $P(y, z)$  can be calculated by (40).

$$u_B(y, z) = \sqrt{\left| \underline{u}_{B_y}(y, z) \right|^2 + \left| \underline{u}_{B_z}(y, z) \right|^2} \quad (40)$$

Finally, for each calculation point with coordinates  $(y, z)$ , the magnetic flux density uncertainty band can be determined from  $B(y, z)$  and  $u_B(y, z)$  values obtained using the equations (39) and (40), as in:

$$B_{band}(y, z) = B(y, z) \pm k \cdot u_B(y, z) = B(y, z) \pm U_B(y, z) \quad (41)$$

where  $k = \sqrt{3}$  denotes the coverage factor and  $U_B(y, z)$  is expanded uncertainty of magnetic flux density at an arbitrary point.

### III. CALCULATION RESULTS

Validation of proposed method is based on four single circuit 400 kV transmission lines, as shown in Fig. 2 and two double circuit overhead transmission lines, shown in Fig. 8.

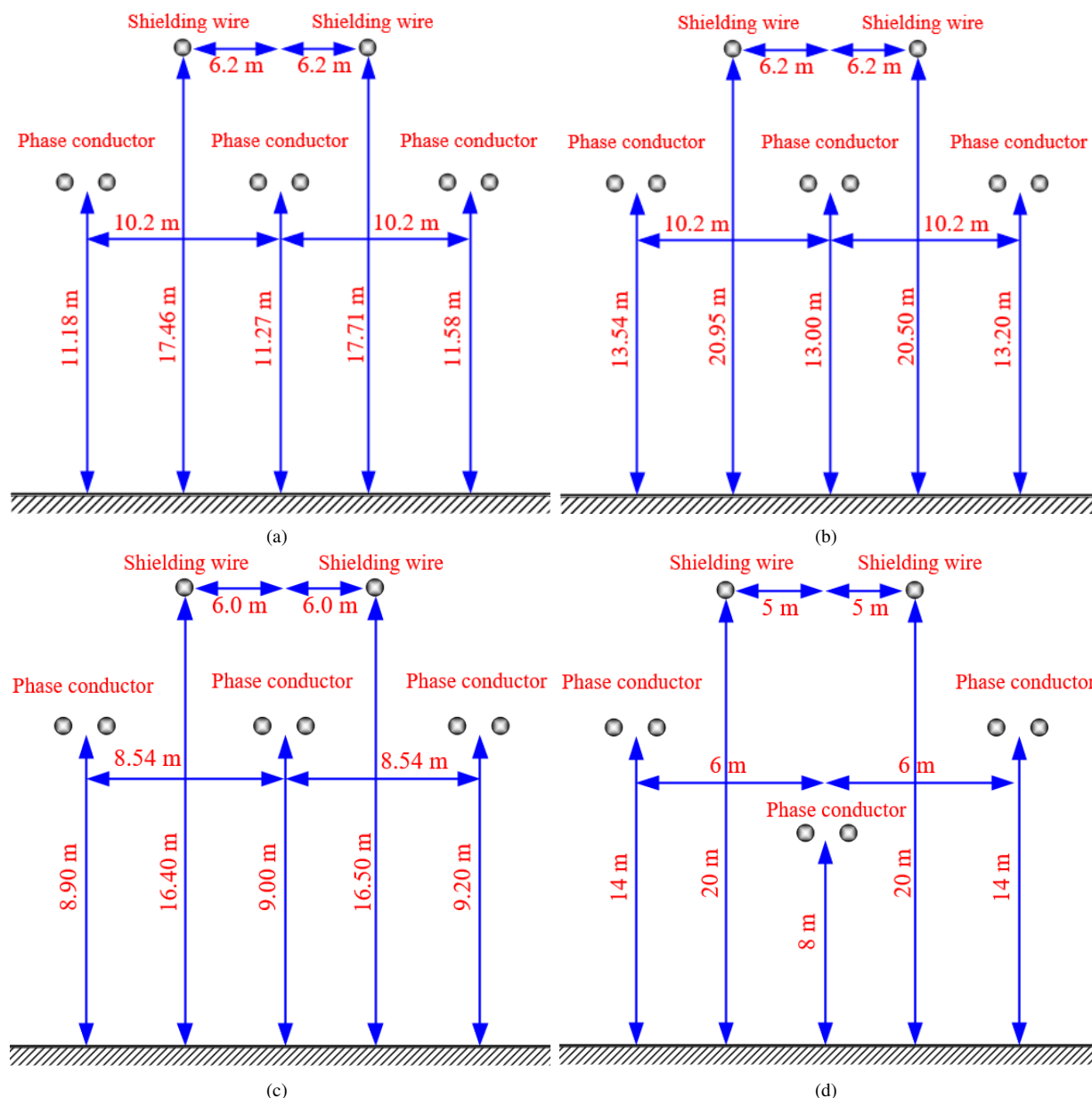


Fig. 2. Geometries of the considered overhead transmission lines: (a) first standard dimensions horizontal configuration 400 kV transmission line [24], (b) second standard dimensions horizontal configuration 400 kV transmission line, (c) reduced dimensions horizontal configuration 400 kV transmission line [28], (d) delta configuration 400 kV transmission line [26].

Electric field intensity and magnetic flux density calculations and determination of corresponding uncertainties are performed on lateral profile in range between  $-40$  m to  $40$  m from central axis of the overhead transmission line. All calculations are performed for a height of  $1$  m above ground surface. The input parameters of the proposed method for evaluating the electric field intensity and magnetic flux density calculation uncertainties in the vicinity of the overhead transmission lines are phase conductors and the shielding wires voltages, currents and heights. Voltage and current intensity values on considered transmission lines are obtained from SCADA system for the period of time during which conductor heights are measured. Based on voltages and current intensities values obtained from SCADA system, it is noticeable that overhead transmission lines were underloaded. Furthermore, in all considered cases balanced conditions are assumed. This implies that the current intensities of all phase

conductors in the three phase system are equal, and the angle between the phases is  $120^\circ$ . The same assumption applies to voltages.

Voltage measurement uncertainty is associated with voltage transformer accuracy class. According to IEC 61869, UCTE Operation Handbook [29], and Grid Code in Bosnia and Herzegovina [30], voltage and current transformers at the accounting points in transmission network must have an accuracy class rating of 0.2. According to IEC 61869, the accuracy class 0.2 for voltage and current measuring transformers corresponds to a maximum measurement error of  $\pm 0.2\%$  [31]–[34]. Conductor height measurements were conducted with Suparule model 600 ultrasonic cable height meter. The instrument accuracy is specified by the manufacturer as  $0.5\% \pm 2$  digits [35].

Electric field intensity and magnetic flux density are phasor quantities defined by magnitude (root mean square value – RMS) and phase angle. The proposed method allows their associated uncertainties to be determined as phasor quantities. On the other hand, the regulations governing the allowed limit values are defined in terms of RMS values. Furthermore, the majority of field measuring instruments register the maximum or RMS field values. Therefore, the RMS value of the total uncertainty is used to validate the results for both considered quantities.

In reality, the exact amounts of phase and amplitude errors of transformers, as well as the error made by the height measuring instrument are not known, but it can be reliably expected to be within the maximum errors as defined by IEC 61869 for measuring transformers and the manufacturer's specification for the height measuring instrument.

The results are obtained for the critical case of calculation, which corresponds to the maximum uncertainty of the input data. The uncertainty of height measurement associated with phase conductors and shielding wires corresponds to 0.5% of the measured value, in all considered cases. For the applied voltages in all considered cases, both capacitive and inductive measuring transformers remain within the maximum error limits determined by the accuracy class [32], [33], which gives an uncertainty of voltage measurement of 0.2% of the measured value in each phase.

When it comes to the uncertainty of current measurement, the situation is somewhat different than with voltage, because the current along the transmission line varies in a much wider range than the voltage. With respect to current measuring transformers, IEC 61869-2 defines the maximum current error limits for the range of primary currents from 5% to 120% of the rated current of current measuring transformers [31]. For the measured value of the phase current, its maximum expected error can be determined using the graph given in Fig. 3. For all considered 400 kV transmission lines, the rated current of the current measuring transformers is 800 A.

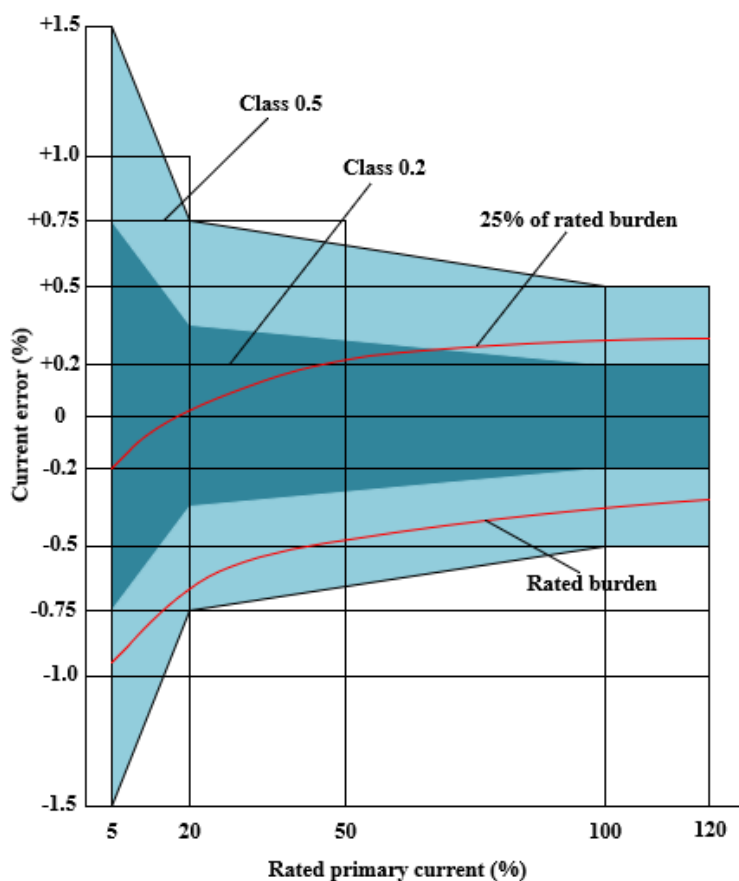


Fig. 3. Limits for accuracy classes 0.2 and 0.5 current transformers according to IEC61689-2 [31], [34].

The expanded measurement uncertainty is shown in all figures. Expression of expanded measurement uncertainty quantifies the uncertainty of the calculation methodology, as well as other influences on input data that are not included in the accuracy classes of measuring transformers and conductor height measuring instruments, and possible deviations of conductors horizontal coordinates from projected. Since all uncertainty values have an equal likelihood of occurring, a uniform probability distribution is assumed for all uncertainty components.

For the overhead transmission line configuration given in Fig. 2a, electric field intensity and magnetic flux density calculation results along with their corresponding uncertainties are shown in Figs. 4a and 4b, respectively. For both the electric field intensity and magnetic flux density calculations, the uncertainty is shown as a band around the calculated values, and the exact values of these quantities are expected to be found within these bands. For the same overhead transmission line configuration, Fig. 2a, the results for the expanded electric field intensity uncertainty and magnetic flux density uncertainty are shown in Figs. 4c and 4d, respectively. RMS values of the measured line-to-line voltage and phase current intensity are 419 kV and 151 A, respectively [24]. Based on the measured phase current intensity, it can be seen that current measuring transformers on this transmission line are loaded with 18.87% of their rated current value. For the calculated load value, from Fig. 3 it is determined that the corresponding maximum expected current measurement uncertainty is 0.38% of the measured value.

From Fig. 4 it can be noted that maximum electric field intensity and magnetic flux density uncertainties can be expected under the transmission line conductors. Uncertainties, and also uncertainty bands which are derived from them are not constant over the considered lateral profile.



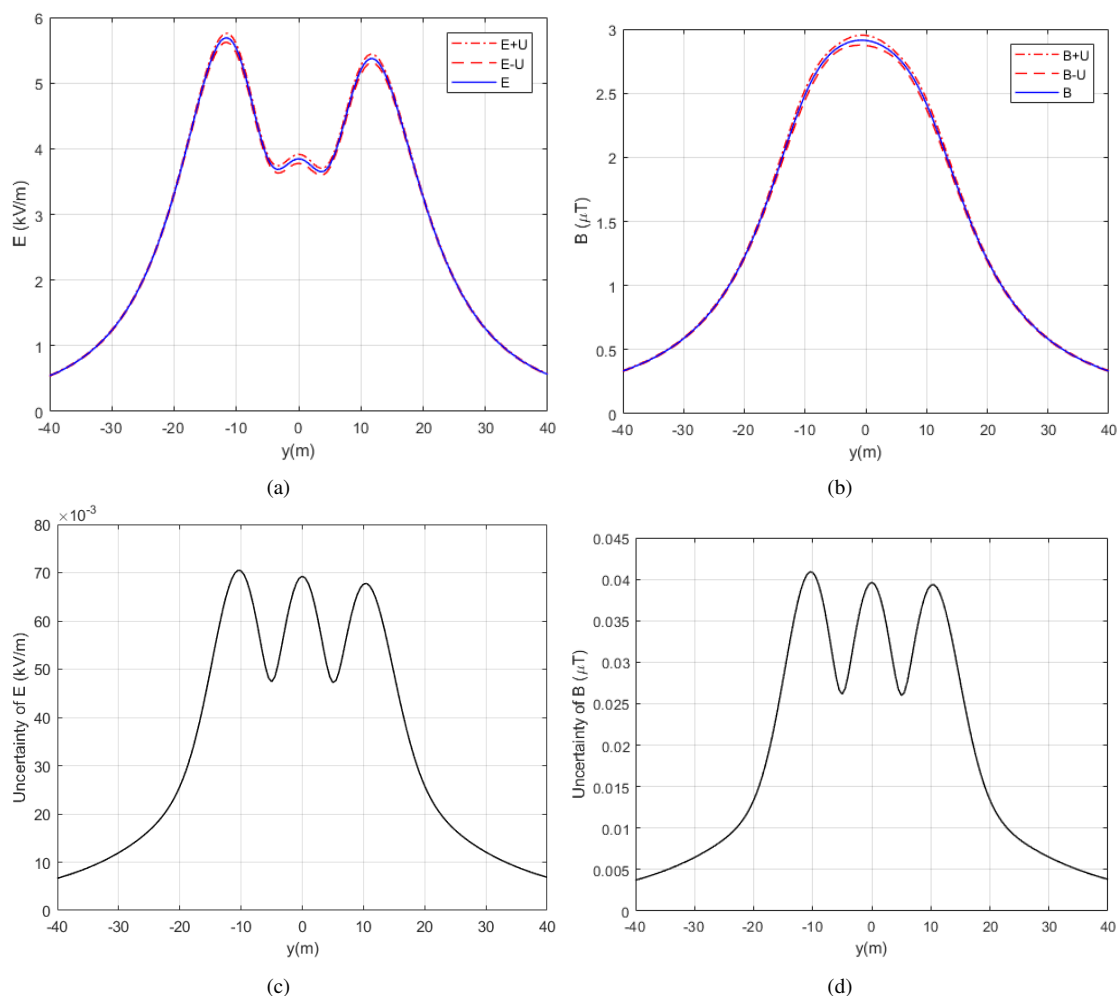


Fig. 4. Calculation results for the first standard dimensions horizontal configuration 400 kV transmission line: (a) electric field intensity with uncertainty band, (b) magnetic flux density with uncertainty band, (c) electric field intensity uncertainty, (d) magnetic flux density uncertainty.

For transmission line given in Fig. 2b, the calculation results are presented in Fig. 5. At the time when conductor heights were measured, applied values of the line-to-line voltage and phase current intensity were 416.7 kV and 193.7 A, respectively.

Comparing this current intensity value with rated current of the current measuring transformers, it can be noted that they were loaded with 24.21% of their rated current value. For this value, from Fig. 3 it is determined that the maximum expected current measurement uncertainty is 0.34%.

By comparing the results shown in Figs. 4 and 5, it can be concluded that despite of similarity in the transmission line parameters, the differences in conductor heights, applied voltage and current intensity values and input parameters uncertainties give rise to different uncertainty results. This further indicates that uncertainty needs to be determined for every different condition even on the same overhead transmission line. Maximum uncertainty values are obtained in the points close to the phase conductor positions.

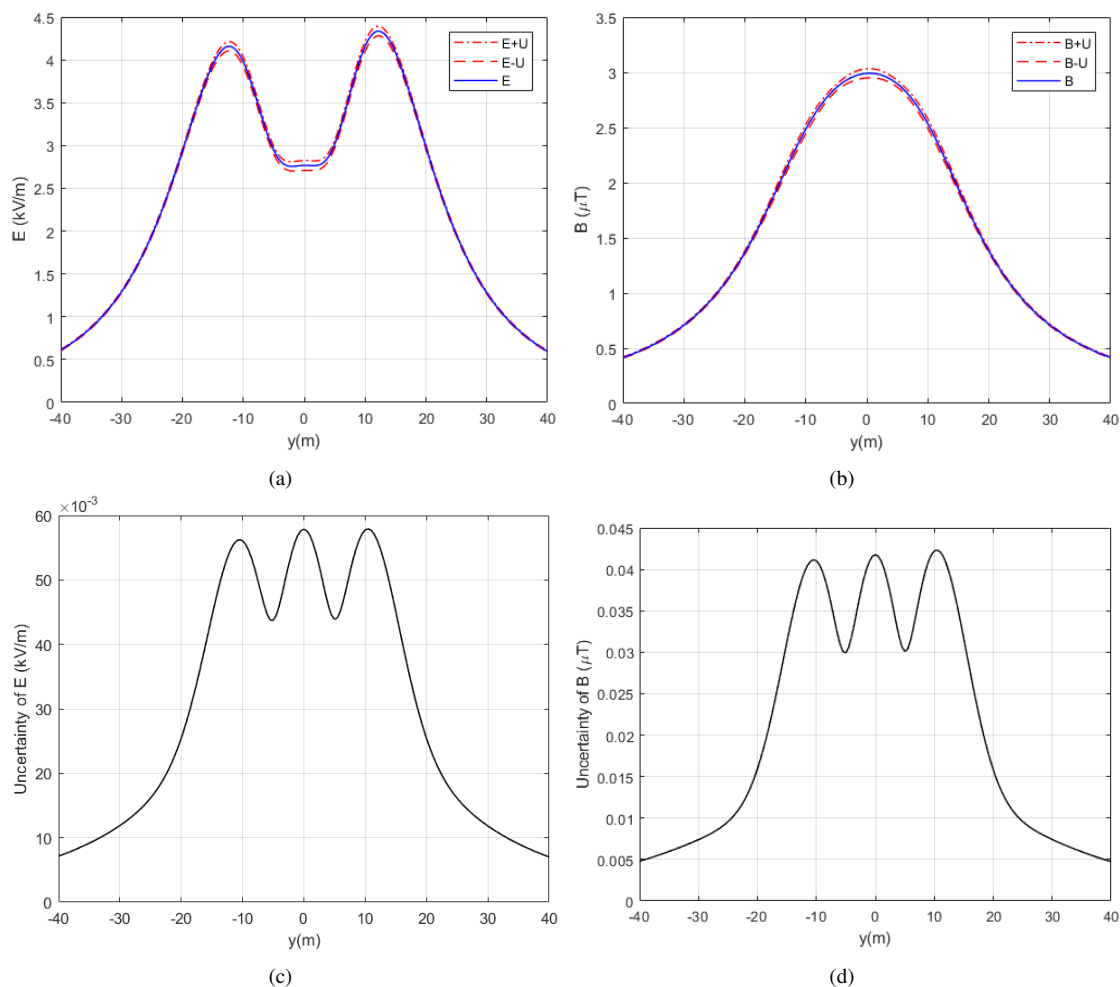


Fig. 5. Calculation results for second standard dimensions horizontal configuration 400 kV transmission line: (a) electric field intensity with uncertainty band, (b) magnetic flux density with uncertainty band, (c) electric field intensity uncertainty, (d) magnetic flux density uncertainty.

Horizontal configuration 400 kV transmission line of reduced dimensions, shown in Fig. 2c is also used for validation of proposed method. For this transmission line configuration, electric field intensity and magnetic flux density uncertainty calculations are made for the measured values of applied line-to-line voltage and phase current of 416 kV and 133.16 A, respectively [28]. At the time of measurement, the current measuring transformers were loaded with 16.65% of their rated current. For this amount of load, it is determined from Fig. 3 that the maximum expected current measurement uncertainty is 0.44%. For these input parameters, electric field intensity and magnetic flux density uncertainty calculations are made, and the obtained results are shown in Fig. 6.

Compared to the previously discussed cases, the results in Fig. 6 show similar variation of uncertainty over the considered lateral profile under the transmission line. However, shorter phase conductor horizontal distances affect the uncertainty variation. Shorter phase conductor horizontal distances produce shorter distances between uncertainty local maximums in the uncertainty function. Also, the differences between other input parameters produce the change in uncertainty magnitudes and consequently in uncertainty bandwidths.

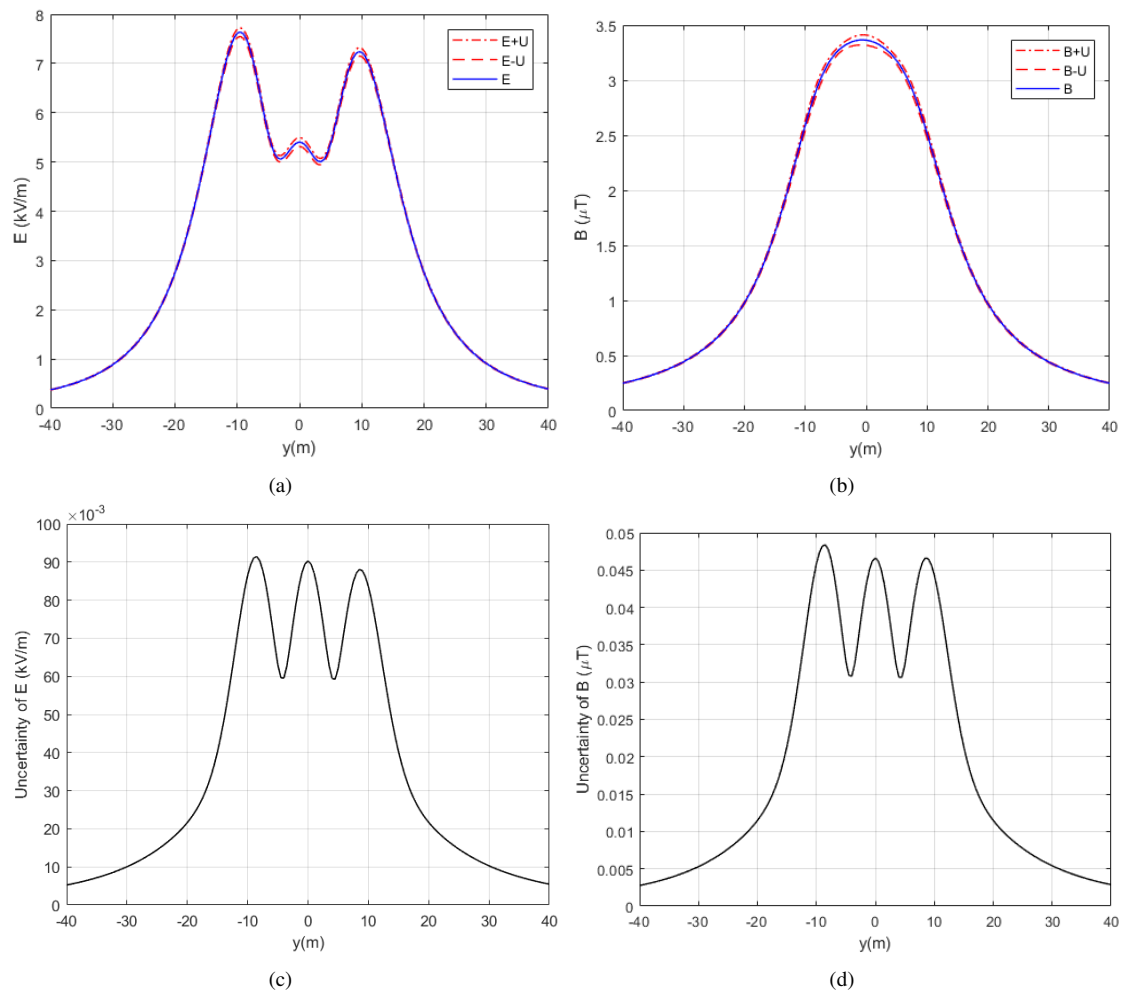


Fig. 6. Calculation results for reduced dimensions horizontal configuration 400 kV transmission line: (a) electric field intensity with uncertainty band, (b) magnetic flux density with uncertainty band, (c) electric field intensity uncertainty, (d) magnetic flux density uncertainty.

For 400 kV overhead transmission line with delta phase conductor configuration, as shown in Fig. 2d, the RMS value of line-to-line voltage and phase current intensity are 440 kV and 100 A, respectively [26]. From these parameters, the rest of calculation input parameters can be determined. Voltage measuring transformers are expected to be within their rated accuracy class which gives 0.2% as voltage measurement uncertainty, and with this load maximum expected current measurement uncertainty is 0.55%. For this case, the calculated electric field intensity and magnetic flux density, the associated uncertainty bands, electric field intensity uncertainty and magnetic flux density uncertainty are shown in Fig. 7.

From Fig. 7 it can be noted that for the overhead transmission line with delta phase conductor configuration, uncertainty variations over the considered lateral profile are similar for both electric field intensity and magnetic flux density. Nevertheless, the influence of phase conductor positions is clearly noticeable from Figs. 7c and 7d.

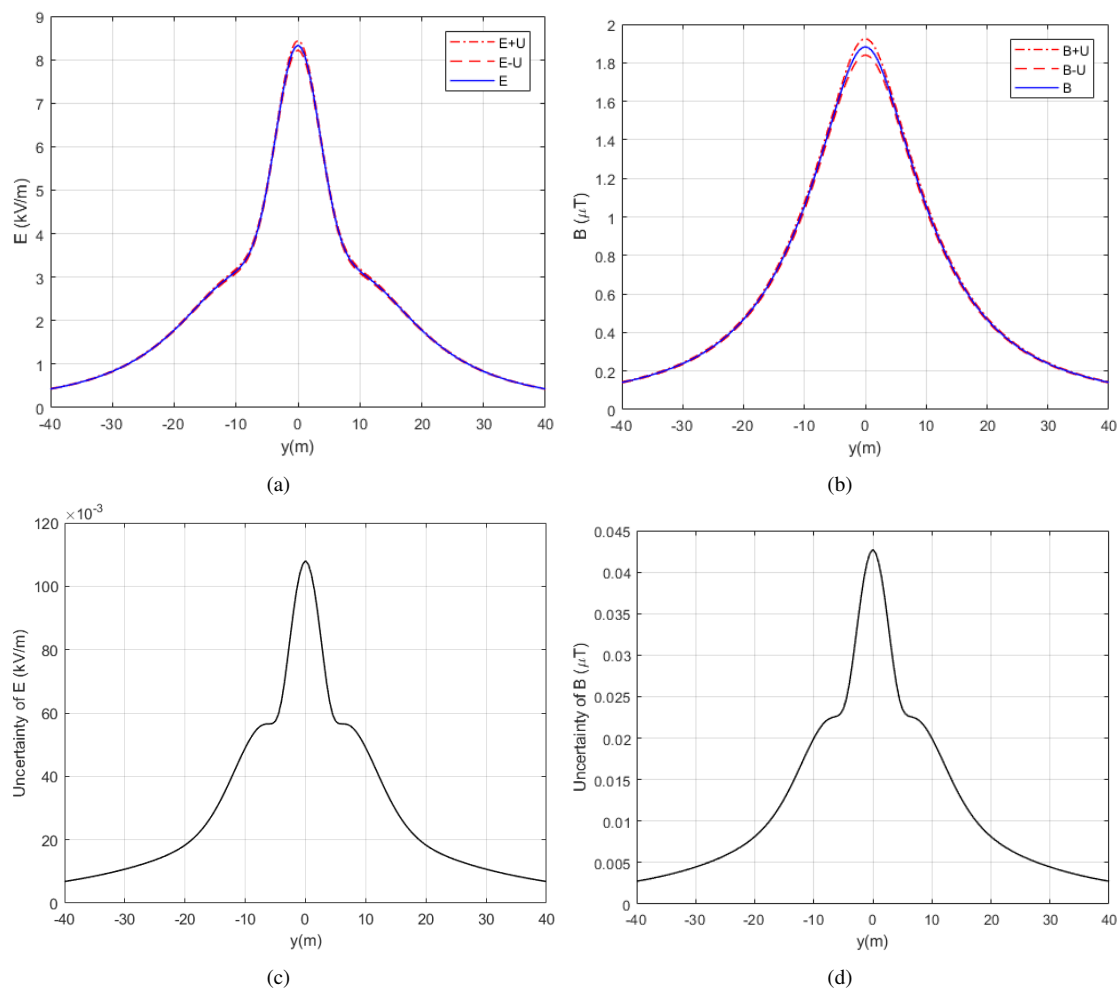


Fig. 7. Calculation results for delta configuration 400 kV transmission line: (a) electric field intensity with uncertainty band, (b) magnetic flux density with uncertainty band, (c) electric field intensity uncertainty, (d) magnetic flux density uncertainty.

Table I displays the maximum values of electric field intensity and magnetic flux density, as well as the maximum values of uncertainty of electric field intensity calculations and uncertainty of magnetic flux density calculations made for four considered overhead transmission line configurations. Also, the maximum ratio of the uncertainty of the electric field intensity calculations to the electric field intensity is determined over the entire lateral profile and presented (as percentage) in Table I. Similarly, the maximum ratio of the uncertainty of the magnetic flux density calculations to the magnetic flux density is also presented in Table I.

TABLE I. MAXIMUM VALUES OF CALCULATED RESULTS FOR THE CONSIDERED TRANSMISSION LINE CONFIGURATIONS

Configuration	$E_{\max}$ (kV/m)	$B_{\max}$ ( $\mu$ T)	$U_{E_{\max}}$ (kV/m)	$U_{B_{\max}}$ ( $\mu$ T)	$(U_E/E)_{\max}$ (%)	$(U_B/B)_{\max}$ (%)
Fig. 2a	5.69	2.91	$70.50 \cdot 10^{-3}$	0.041	1.80	1.73
Fig. 2b	4.33	2.99	$57.93 \cdot 10^{-3}$	0.042	2.09	1.76
Fig. 2c	7.64	3.36	$91.45 \cdot 10^{-3}$	0.048	1.67	1.77
Fig. 2d	8.33	1.88	$108.08 \cdot 10^{-3}$	0.043	1.59	2.27

The proposed method is not limited to the single circuit transmission lines only, but can be also applied for uncertainty of electric field intensity and magnetic flux density calculation in the case of multi circuit transmission lines. The proposed method is validated on two double circuit transmission

lines given in Fig. 8.

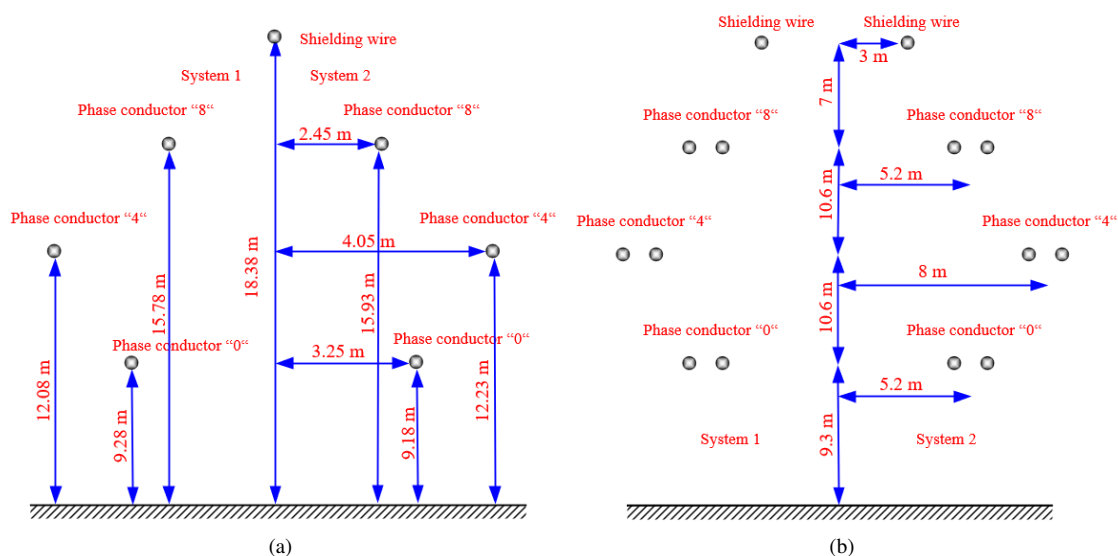


Fig. 8. Geometries of the considered double circuit transmission lines: (a) 110 kV transmission line, (b) 400 kV transmission line [36].

First considered case corresponds to two independent 110 kV transmission lines which in one part of their route are led together on a common transmission line tower, and make double circuit transmission line. This configuration is shown in Fig. 8a. At the time when height measurements are made, RMS values of line-to-line voltages and phase current intensities are obtained from SCADA system. For the first transmission line RMS values of line-to-line voltages and phase currents intensity are 114.85 kV and 42.96 A, respectively, whilst for the second transmission line, they are 115.1 kV and 31.76 A, respectively.

For the considered 110 kV transmission lines, the rated current value of the current measuring transformers is 600 A. Applying the same principles as in previously considered cases, the maximum expected voltage and current intensity measurement uncertainties are determined. For both transmission lines, the voltage measurement uncertainty is 0.2%, while the maximum expected current intensity measurement uncertainties are 0.69% and 0.74% for the first and second transmission line, respectively.

Corresponding electric field intensity, magnetic flux density and their respective uncertainties calculation results are shown in Fig. 9. From the results given in Fig. 9 it can be noted how differences in the input parameters between the different circuits on multiple circuit transmission line affect the uncertainty results. In the case of electric field intensity, input parameters are only slightly different between the two transmission lines and thus, electric field intensity and uncertainty functions are almost symmetrical in regards to the axis of the transmission line, as shown in Figs. 9a and 9c. When it comes to magnetic flux density, situation is somewhat different. Here, a larger difference in the current intensity values has a significant impact on the calculation results and corresponding uncertainties, as it can be seen in Figs. 9b and 9d.

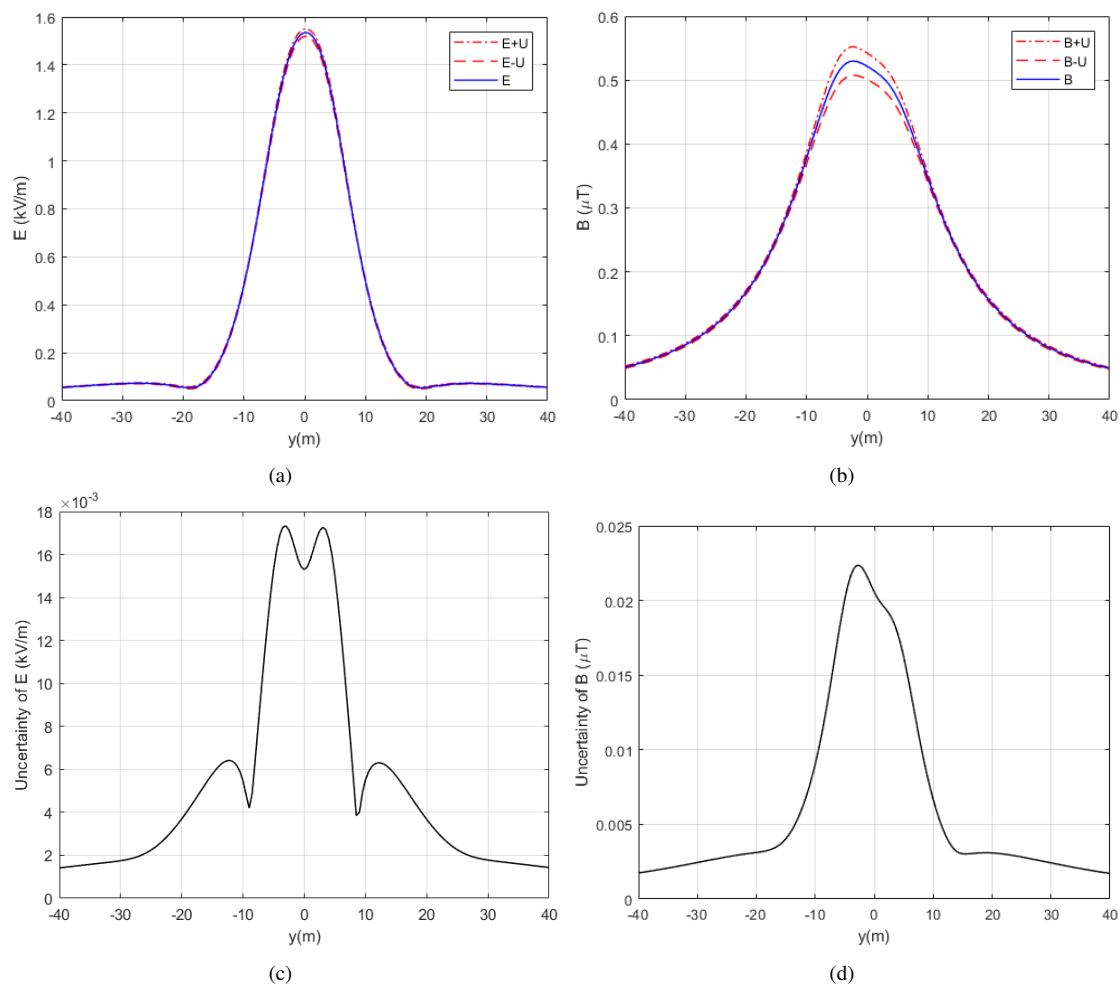


Fig. 9. Calculation results for double circuit 110 kV transmission line: (a) electric field intensity with uncertainty band, (b) magnetic flux density with uncertainty band, (c) electric field intensity uncertainty, (d) magnetic flux density uncertainty.

For the double circuit overhead transmission of rated voltage 400 kV line given in Fig. 8b, the RMS value of the line-to-line voltage in both circuits was 422.97 kV [36], and calculations are made under the assumption that the current intensity is 800 A in both of them. For this voltage and current intensity values expected maximum voltage and current measurement uncertainties are determined as 0.2% according to previously discussed procedure. For this case, calculation results are shown in Fig. 10. The electric field intensity, magnetic flux density and their respective calculation uncertainties results are shown in Fig. 10.

For the multi circuit overhead transmission lines shown in Fig. 8, the maximum calculated values of electric field intensity, magnetic flux density, electric field intensity uncertainty and magnetic flux density uncertainty are given in Table II. The maximum ratio of the uncertainty of the electric field intensity calculation to the electric field intensity determined over the entire lateral profile and presented (as percentage) is given in Table II. Furthermore, the maximum ratio of the uncertainty of the magnetic flux density to the magnetic flux density is presented in Table II.

Fig. 10 shows that double circuit transmission line configuration with completely symmetrical geometry, voltage and current intensity values on both circuits will produce uncertainty results which are symmetrical around the axis of the transmission line.

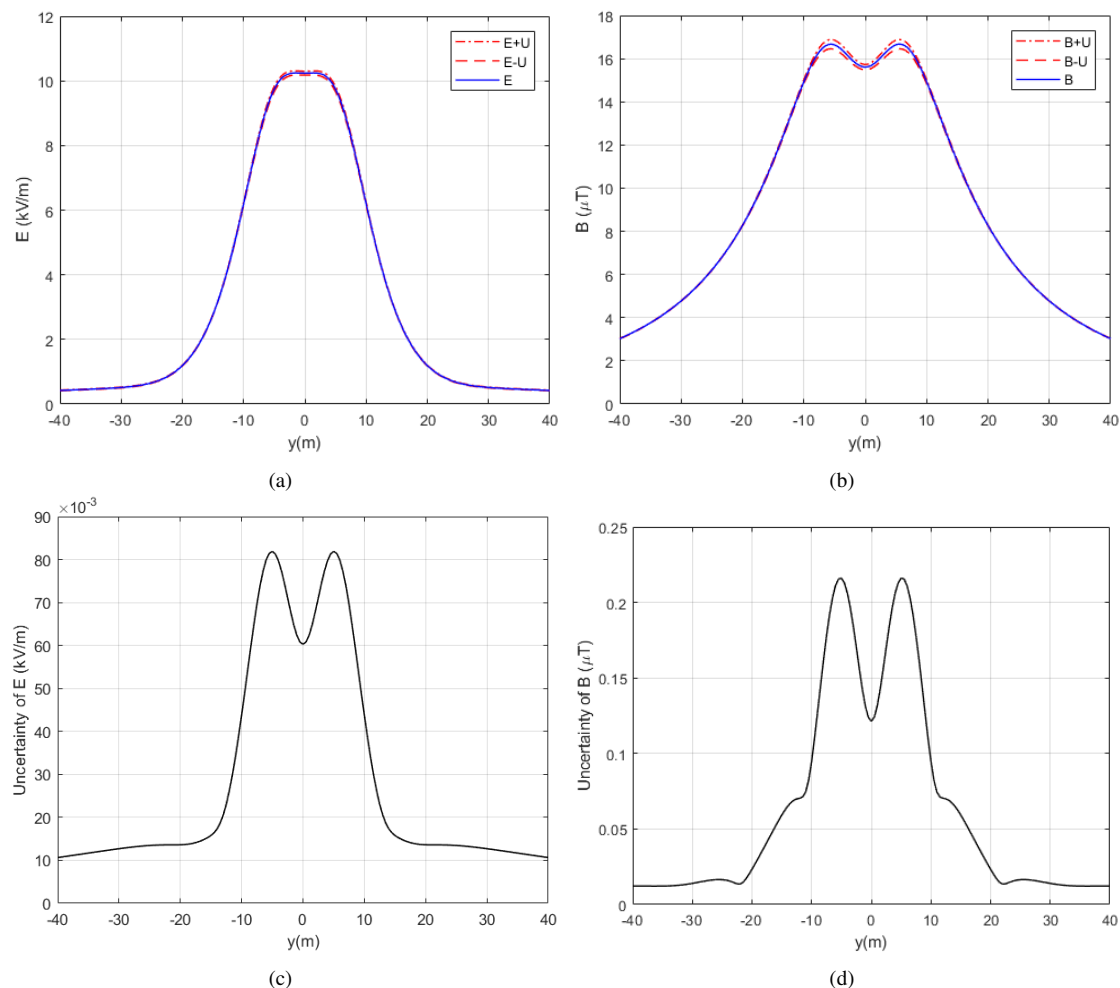


Fig. 10. Calculation results for double circuit 400 kV transmission line: (a) electric field intensity with uncertainty band, (b) magnetic flux density with uncertainty band, (c) electric field intensity uncertainty, (d) magnetic flux density uncertainty.

TABLE II. MAXIMUM VALUES OF CALCULATED RESULTS FOR CONSIDERED DOUBLE CIRCUIT TRANSMISSION LINE CONFIGURATIONS

Configuration	$E_{\max}(\text{kV/m})$	$B_{\max}(\mu\text{T})$	$U_{E_{\max}}(\text{kV/m})$	$U_{B_{\max}}(\mu\text{T})$	$(U_E/E)_{\max}(\%)$	$(U_B/B)_{\max}(\%)$
Fig. 8a	1.53	0.53	$17.33 \cdot 10^{-3}$	0.02	7.95	4.23
Fig. 8b	10.24	16.67	$81.90 \cdot 10^{-3}$	0.22	2.53	1.29

It can be observed from Tables I and II that there are some differences between the maximum ratio of the electric field intensity calculation uncertainty to the electric field intensity and the corresponding ratio for the magnetic flux density. The reason for these differences can be found in measurement errors associated with voltage and current measuring transformers. As it is discussed earlier in this section, voltage and current measurements uncertainties correspond to expected maximum error limits of measuring transformers. In all considered cases, the voltage measurements are made with the same uncertainty. On the other hand, the current measurement uncertainty is significantly affected by the deviations of the applied phase current intensities from the rated currents of the current measuring transformers. Voltage and current measurements uncertainties have significant impact on the electric field intensity and magnetic flux density calculation uncertainties. When determining the electric field intensity calculation uncertainty, the uncertainty of the voltage measurements is taken into account

indirectly via the previously determined fictitious point charge phasors calculation uncertainty. On the contrary, the current measurement uncertainty directly affects the magnetic flux density calculation uncertainty.

The results given in Figs. 4 - 7 and Figs. 9 - 10 show that the proposed method is able to calculate electric field intensity and magnetic flux density calculation uncertainty for all considered overhead transmission line configurations, applied voltage and current intensity values over the entire considered lateral profile. The results show that the proposed method can be used for accurately determination of electric field intensity and magnetic flux density calculation uncertainties, irrespective of geometric description of overhead transmission lines, applied voltage and current intensity values and input parameters uncertainties.

It can be noted that both, electric field intensity and magnetic flux density uncertainties, vary not only with input parameters (conductor heights, voltage and current intensity values) but also with the location of the observation point. They have different value in every point over the considered lateral profile.

#### IV. CONCLUSION

This paper proposes a algorithm for determination of uncertainty of electric field intensity and magnetic flux density calculation in the vicinity of overhead transmission lines. The presented method is based on the law of propagation of uncertainty defined in GUM, the CSM method for determining the electric field intensity, and the BS law based method for the calculation of magnetic flux density. The calculation results on real configurations of overhead transmission lines show that by applying the proposed algorithm, the uncertainty of the calculation of electric field intensity and magnetic flux density can be precisely and reliably determined, at all points of interest.

Growing public concern about the impact of overhead transmission lines on the environment is one of the challenges facing electric power transmission companies. That is why determining the value of the electric field intensity and magnetic flux density generated by the overhead transmission lines in operation or the expected field values of the lines whose construction is planned is becoming increasingly important. Considering that the comparison of the calculated electric field intensity and magnetic flux density values with the prescribed limit values requires the expression of expanded uncertainty of the obtained results, it is of crucial importance to determine calculation uncertainty as precisely as possible. This is especially important when the calculated values are close to the limit values, as defined by the regulations.

#### REFERENCES

- [1] J. S. Acosta and M. C. Tavares, "Optimal selection and positioning of conductors in multi-circuit overhead transmission lines using evolutionary computing," *Electric Power Systems Research*, vol. 180, p. 106174, 2020.
- [2] A. L. Paganotti, R. R. Saldanha, A. C. Lisboa, M. M. Afonso, M. Q. Melo, and M. A. O. Schroeder, "Methodology for minimizing electric field at ground level from transmission lines using sensitivity analysis," *Journal of Microwaves, Optoelectronics and Electromagnetic Applications*, vol. 20, no. 4, pp. 702–713, 2021.
- [3] I. Duane, M. Afonso, M. Schroeder, S. Gonçalves, A. Paganotti, and R. Saldanha, "A New Strategy for Optimizing HSIL Transmission Lines," *Journal of Control, Automation and Electrical Systems*, vol. 31, 07 2020.
- [4] J. S. Acosta and M. C. Tavares, "Methodology for optimizing the capacity and costs of overhead transmission lines by modifying their bundle geometry," *Electric Power Systems Research*, vol. 163, pp. 668 – 677, 2018, advances in HV Transmission Systems.

- [5] E. Lunca, S. Ursache, and A. Salceanu, "Computation and analysis of the extremely low frequency electric and magnetic fields generated by two designs of 400 kv overhead transmission lines," *Measurement*, vol. 124, pp. 197–204, 2018.
- [6] A. Amoon, C. Crespi, A. Ahlbom, M. Bhatnagar, I. Bray, K. Bunch, J. Clavel, M. Feychting, D. Hémon, C. Johansen, C. Kreis, C. Malagoli, F. Marquant, C. Pedersen, O. Raaschou-Nielsen, M. Röösl, B. Spycher, M. Sudan, J. Swanson, and L. Kheifets, "Proximity to overhead power lines and childhood leukaemia: an international pooled analysis," *British Journal of Cancer*, vol. 119, 05 2018.
- [7] T. Samaras, N. Leitgeb, A. Auvinen, H. Danker-Hopfe, K. Hansson Mild, M.-O. Mattsson, H. Norppa, G. Rubin, M. R. Scarfi, J. Schüz, Z. Sienkiewicz, and O. Zeni, *SCENIHR (Scientific Committee on Emerging and Newly Identified Health Risks), Potential health effects of exposure to electromagnetic fields (EMF), 27 January, 2015*, 01 2015.
- [8] J. Lin, R. Saunders, K. Schulmeister, P. Söderberg, B. Stuck, A. Swerdlow, M. Taki, B. Veyret, G. Ziegelberger, M. Repacholi, R. Matthes, A. Ahlbom, K. Jokela, and C. Roy, "ICNIRP Guidelines for limiting exposure to time-varying electric and magnetic fields (1 Hz to 100 kHz)." *Health Phys.*, vol. 99, 01 2010.
- [9] "IEC 61786-2:2014 - Measurement of DC magnetic, AC magnetic and AC electric fields from 1 Hz to 100 kHz with regard to exposure of human beings - Part 2: Basic standard for measurements," *International Electrotechnical Commission*, 2014.
- [10] A. Tzinevrakis, D. Tsanakas, and E. Mimos, "Electric field analytical formulas for single-circuit power lines with a horizontal arrangement of conductors," *IET Generation, Transmission & Distribution*, vol. 3, pp. 509 – 520, 07 2009.
- [11] A. Geri, A. Locatelli, and G. M. Veca, "Magnetic fields generated by power lines," *IEEE Transactions on Magnetics*, vol. 31, no. 3, pp. 1508–1511, 1995.
- [12] F. Muñoz, J. Aguado, F. Martín, J. López, A. Rodríguez, J. García, A. Treitero, and R. Molina, "An intelligent computing technique to estimate the magnetic field generated by overhead transmission lines using a hybrid GA-Sx algorithm," *International Journal of Electrical Power & Energy Systems*, vol. 53, pp. 43–53, 2013.
- [13] D. Rabah, C. Abdelghani, and H. Abdechafik, "Efficiency of some optimization approaches with the Charge simulation method (CSM) for calculating the electric field under EHV power lines," *IET Generation, Transmission & Distribution*, vol. 11, 03 2017.
- [14] J. Brandao Faria and M. Almeida, "Accurate calculation of magnetic-field intensity due to overhead power lines with or without mitigation loops with or without capacitor compensation," *IEEE Transactions on Power Delivery*, vol. 22, pp. 951 – 959, 05 2007.
- [15] M. Grbic, D. Salamon, and J. Mikulović, "Analysis of influence of measuring voltage transformer ratio error on single-circuit overhead power line electric field calculation results," *Electric Power Systems Research*, vol. 166, pp. 232–240, 01 2019.
- [16] *JCGM 100:2008 - Guide to the expression of uncertainty in measurement*.
- [17] B. Siebert, "Uncertainty in radiation dosimetry: basic concepts and methods," *Radiation protection dosimetry*, vol. 121, no. 1, pp. 3–11, 2006.
- [18] C. F. Carobbi, S. Lalléchère, and L. R. Arnaut, "Review of uncertainty quantification of measurement and computational modeling in emc part i: Measurement uncertainty," *IEEE Transactions on Electromagnetic Compatibility*, vol. 61, no. 6, pp. 1690–1698, 2019.
- [19] B. Vulevic, P. Osmokrovic, and D. Kovacevic, "Survey of radiofrequency radiation levels around gsm base stations and evaluation of measurement uncertainty," *Nuclear Technology and Radiation Protection*, vol. 26, pp. 214–217, 12 2011.
- [20] I. Ztoupis, I. Gonos, and I. Stathopoulos, "Uncertainty evaluation in the measurement of power frequency electric and magnetic fields from ac overhead power lines," *Radiation protection dosimetry*, vol. 157, 05 2013.
- [21] B. Vulević and P. Osmokrović, "Evaluation of uncertainty in the measurement of environmental electromagnetic fields," *Radiation Protection Dosimetry*, vol. 141, no. 2, pp. 173–177, 05 2010.
- [22] M. Grbic, J. Mikulović, and D. Salamon, "Influence of measurement uncertainty of overhead power line conductor heights on electric and magnetic field calculation results," *International Journal of Electrical Power & Energy Systems*, vol. 98, pp. 167–175, 06 2018.
- [23] "IEEE Standard Procedures for Measurement of Power Frequency Electric and Magnetic Fields from AC Power Lines," *IEEE Std 644-2019 (Revision of IEEE Std 644-2008)*, pp. 1–40, 2020.
- [24] A. Mujezinović, A. Čarsimamović, S. Čarsimamović, A. Muharemović, and I. Turković, "Electric field calculation around of overhead transmission lines in bosnia and herzegovina," in *2014 International Symposium on Electromagnetic Compatibility*, pp. 1001–1006, 2014.
- [25] K. B. Petersen and M. S. Pedersen, "The matrix cookbook," nov 2012, version 20121115. [Online]. Available: <http://www2.compute.dtu.dk/pubdb/pubs/3274-full.html>

- [26] A. Alihodzic, A. Mujezinovic, and E. Turajlic, "Electric and Magnetic Field Estimation Under Overhead Transmission Lines Using Artificial Neural Networks," *IEEE Access*, vol. 9, pp. 105 876–105 891, 2021.
- [27] J. Salari, A. Mpalantinos, and J. Silva, "Comparative analysis of 2-d and 3-d methods for computing electric and magnetic fields generated by overhead transmission lines," *IEEE Transactions on Power Delivery*, vol. 24, pp. 338 – 344, 02 2009.
- [28] A. Carsimamovic, A. Mujezinovic, Z. Bajramovic, I. Turkovic, and M. Kosarac, "Low frequency electric field radiation level around high-voltage transmission lines and impact of increased voltage values on the corona onset voltage gradient," *Nuclear Technology and Radiation Protection*, vol. 33, 06 2018.
- [29] "UCTE Operation Handbook Appendix 1 Chapter A: Scheduling of Power Exchange, 2016," 2016.
- [30] "Grid Code," *Independent System Operator in Bosnia and Herzegovina*, 2019.
- [31] "IEC 61869-2:2012 - Instrument transformers - Part 2: Additional requirements for current transformers," *International Electrotechnical Commission*, 2012.
- [32] "IEC 61869-3:2011 - Instrument transformers - Part 3: Additional requirements for inductive voltage transformers," *International Electrotechnical Commission*, 2011.
- [33] "IEC 61869-5:2011 Instrument transformers - Part 5: Additional requirements for capacitor voltage transformers," *International Electrotechnical Commission*, 2011.
- [34] *ABB Instrument Transformers Application Guide*, 2015.
- [35] SUPARULE, "Cable height meter - technical information," 2021. [Online]. Available: <https://www.suparule.com/products/cable-height-meter>
- [36] A. Carsimamovic, A. Mujezinovic, Z. Bajramovic, I. Turkovic, N. Dautbasic, and M. Košarac, "Impact of tower arrangement on the mitigation of the electric field intensity on the high-voltage conductors," in *2019 International Symposium on Electromagnetic Compatibility - EMC EUROPE*, pp. 76–81, 2019.